Inorg. Chem. **2006**, *45*, 4801–4810

Diversity of Coordination Architecture of Metal 4,5-Dicarboxyimidazole

Rui-Qin Fang and Xian-Ming Zhang*

School of Chemistry & Material Science, Shanxi Normal University, Linfen 041004, P. R. China

Received December 8, 2005

Seven complexes of metal 4,5-dicarboxyimidazole acid (H_3dcbi), namely, $[Cd(H_2dcbi)_2(H_2O)_3]\cdot H_2O$ (**1**·α), $[Cd(H_2dcbi)_2(H_2O)_2]\cdot 2H_2O$ (**1**·β), $[Cd(H_2dcbi)_2(H_2O)_2]\cdot 2H_2O$ (**1**·γ), $[Cd(H_2dcbi)_2(H_2O)_2]$ (**2**), [Cd(Hdcbi)(H$_2$O)] (**3**), $[Cd_5(Hdcbi)_2(dcbi)_2(H_2O)]\cdot XH_2O$ (**4**), $[Cd_2(Hdcbi)(C_2O_4)]$ (**5**), $[Ag_5(Hdcbi)_2(CN)]$ (**6**), and [Mn(Hdcbi)(H$_2$O)] (**7**), have been hydro(solvo)thermally synthesized by fine control over synthetic conditions such as stoichiometry, solvent, and pH value. X-ray single-crystal structural analyses reveal that they have rich structural chemistry ranging from mononuclear (**1**), one-dimensional (**2**), and two-dimensional (**3** and **7**) to three-dimensional (**4**–**6**), among which **1** crystallizes in three types (α, β, and γ) of polymorphs. Seven coordination modes of $H_n$dcbi ranging from monodentate to μ_5 have been observed, among which four modes are found first. The coordination geometries of the Cd(II) sites vary from five-coordinate trigonal bipyramid and square pyramid, six-coordinate octahedron to seven-coordinate pentagonal bipyramid. Analyses of the synthetic conditions and structures of the Cd(II) complexes show that the influences of the solvent and the metal-to-ligand molar ratio are very important to the products and coordination modes of $H_n$dcbi (n = 0, 1, 2). Studies of the coordination modes of $H_n$dcbi and the structures of the Cd(II) complexes also reveal that the singly deprotonated H_2dcbi generally coordinates in the monodentate imidazole-N or N,O-chelate mode to result in mononuclear structures, the doubly deprotonated Hdcbi coordinates in the μ_2, μ_3, or μ_4 mode to generate one-dimensional or two-dimensional structures, and the triply deprotonated dcbi can coordinate in the μ_5 mode to form three-dimensional structures. The cyanide was in situ formed via C–C bond cleavage of acetonitrile during the preparation of **6**, which adopts a rare μ_4-*k*C,*k*C:*k*N,*k*N mode to bridge four Ag(I) ions. The microporous three-dimensional framework of **4** is maintained after the removal of the guest molecules. Compounds **1**–**5** show strong violet emissions with maxima around 380 nm, tentatively attributed to the ligand-centered transition.

Introduction

Design of a metal−organic framework via deliberate selection of metals and multifunctional ligands is one of the most attractive topics because of the fascinating structural diversity and potential applications in catalysis, chirality, conductivity, luminescence, magnetism, sensors, nonlinear optics, and porosity.[1−5] The organic ligands containing N and O donors offer great potential for fine control over coordination architectures.[6,7] Pyrazole-3,5-dicarboxylic acid has been widely used to synthesize various coordination polymers because it has very flexible coordination modes.[8] Similar to pyrazole-3,5-dicarboxylic acid, 4,5-dicarboxy-

* To whom correspondence should be addressed. Fax/Phone: +86 357 2051402. E-mail: zhangxm@dns.sxnu.edu.cn.

(1) (a) Yaghi, O. M.; Li, H.; Davis, C. D.; Groy, T. L. *Acc. Chem. Res.* **1998**, *31*, 474. (b) Blake, A. J.; Champness, N. R.; Hubberstey, P.; Li, W. S.; Withersby, M. A.; Schröder, M. *Coord. Chem. Rev.* **1999**, *183*, 117. (c) Hagrman, P. J.; Hagrman, D.; Zubieta, J. *Angew. Chem., Int. Ed.* **1999**, *38*, 2638. (d) Fujita, M. *Acc. Chem. Res.* **1998**, *32*, 53. (e) Moulton, B.; Zaworotko, M. J. *Chem. Rev.* **2001**, *101*, 1629. (f) Batten, S. R.; Robson, R. *Angew. Chem., Int. Ed.* **1998**, *37*, 1460. (g) Carlucci, L.; Ciani, G.; Proserpio, D. M. *Coord. Chem. Rev.* **2003**, *246*, 247. (h) Eddaoudi, M.; Moler, D. B.; Li, H.; Chen, B.; Reineke, T. M.; O'Keeffe, M. and Yaghi, O. M. *Acc. Chem. Res.* **2001**, *34*, 319. (i) Evans, O. R.; Lin, W. *Acc. Chem. Res.* **2002**, *35*, 511.

(2) (a) Chui, S. S. Y.; Lo, S. M. F.; Charmant, J. P. H.; Orpen, A. G.; Williams, I. D. *Science* **1999**, *283*, 1148. (b) Noro, S. I.; Kitagawa, S.; Kondo, M.; Seki, K. *Angew. Chem., Int. Ed.* **2000**, *39*, 2082. (c) Chae, H. K.; Eddaoudi, M.; Kim, J.; Hauck, S. I.; Hartwig, J. F.; O'Keeffe, M.; Yaghi, O. M. *J. Am. Chem. Soc.* **2001**, *123*, 11482.

(3) (a) Serre, C.; Millange, F.; Thouvenot, C.; Nogues, M.; Marsolier, G.; Louer, D.; Ferey, G. *J. Am. Chem. Soc.* **2002**, *124*, 13519. (b) Sasa, M.; Tanaka, K.; Bu, X. H.; Shiro, M.; Shionoya, M. *J. Am. Chem. Soc.* **2001**, *123*, 10750. (c) Bu, X.-H.; Tong, M.-L.; Chang, H.-C.; Kitagawa, S.; Batten, S. R. *Angew. Chem., Int. Ed.* **2003**, *43*, 192. (d) Fang, G.; Zhu, M.; Xue, J.; Sun, Y.; Wei, S.; Qiu, R.; Xu, Q. *Angew. Chem., Int. Ed.* **2005**, 44, 3845.

(4) (a) Gao, E.-Q.; Yue, Y.-F.; Bai, S.-Q.; He, Z.; Yan, C.-H. *J. Am. Chem. Soc.* **2004**, *126*, 1419. (b) Imai, H.; Inoue, K.; Kikuchi, K.; Yoshida, Y.; Ito, M.; Sunahara, T.; Onaka, S. *Angew. Chem.* **2004**, *116*, 5736.

(5) (a) Evans, O. R.; Xiong, R. G.; Wang, Z.; Wong, G. K.; Lin, W. *Angew. Chem., Int. Ed*. **1999**, *38*, 536. (b) Seo, J. S.; Whang, D.; Lee, H.; Jun, S. I.; Oh, J.; Jeon, Y. J.; Kim, K. *Nature* **2000**, *404*, 982. (c) Xiong, R. G.; You, X. Z.; Abrahams, B. F.; Xue, Z.; Che, C. M. *Angew. Chem., Int. Ed.* **2001**, *40*, 4422.

10.1021/ic052099m CCC: $33.50
Published on Web 05/13/2006

Scheme 1. Possible Coordination Modes of $H_n$dcbi ($n = 0-2$)

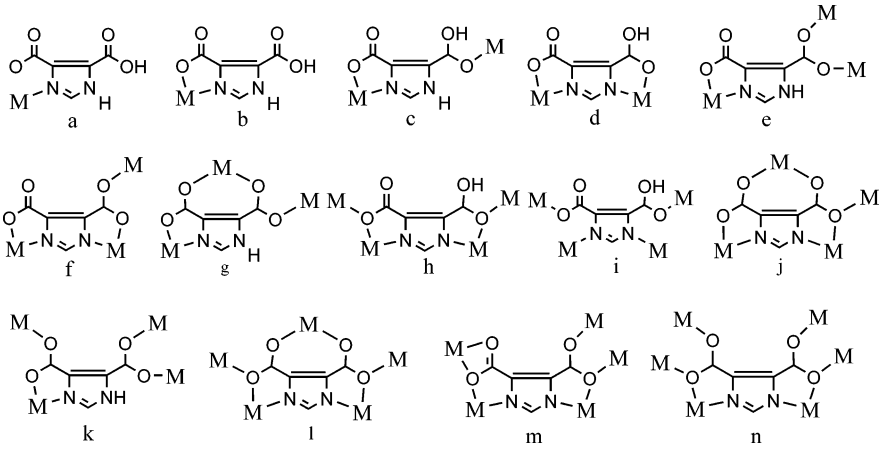

imidazole (H_3dcbi) also has six potential donor atoms, and it can remove one to three hydrogen atoms forming $H_n$dcbi ($n = 0$, 1, 2) species. Thus one may expect that the deprotonated $H_n$dcbi ($n = 0$, 1, 2) exhibit flexible coordination modes. Scheme 1 shows thirteen possible coordination modes of $H_n$dcbi. However, the coordination chemistry of $H_n$dcbi is relatively less explored and only a few complexes containing $H_n$dcbi ligand have been structurally characterized.[9] In the work, we explore the influences of various hydro(solvo)thermal parameters on the products and coordination modes of $H_n$dcbi and report herein seven metal complexes, namely, $[Cd(H_2dcbi)_2(H_2O)_3]\cdot H_2O$ (**1**·α), $[Cd(H_2dcbi)_2(H_2O)_2]\cdot 2H_2O$ (**1**·*β*), $[Cd(H_2dcbi)_2(H_2O)_2]\cdot 2H_2O$ (**1**·*γ*), $[Cd(H_2dcbi)_2(H_2O)_2]$ (**2**), [Cd(Hdcbi)(H$_2$O)] (**3**), $[Cd_5(Hdcbi)_2(dcbi)_2(H_2O)]\cdot XH_2O$ (**4**), $[Cd_2(Hdcbi)(C_2O_2)]$ (**5**), $[Ag_5(Hdcbi)_2(CN)]$ (**6**), and [Mn(Hdcbi)(H$_2$O)] (**7**).

Experimental Section

Materials and Methods. All the starting materials were purchased commercially, were reagent grade, and were used without further purification. Elemental analyses were performed on a Perkin-Elmer 240 elemental analyzer. The FT-IR spectra were recorded from KBr pellets in range of 400−4000 cm^{-1} on a Nicolet 5DX spectrometer. The emission/excitation spectra were recorded on a Perkin-Elmer LS50B fluorescence spectrophotometer. Thermal gravimetric analysis (TGA) of **4** was performed under a static air atmosphere using a Perkin-Elmer 7 thermogravimetric analyzer with a heating rate of 10 °C min^{-1}. XRPD data were recorded in a Bruker D8 ADVANCE X-ray powder diffractometer.

$[Cd(H_2dcbi)_2(H_2O)_3]\cdot H_2O$ (1·α). A mixture of $CdCl_2\cdot 2.5H_2O$ (0.068 g, 0.20 mmol), H_3dcbi (0.046 g, 0.30 mmol), $Na_2SiO_3\cdot 9H_2O$ (0.057 g, 0.20 mmol), and deionized water (7 mL) was stirred, and the it was transferred to and sealed in a 15 mL Teflon-lined bomb, which was heated to 140 °C for 4 days. After the mixture was cooled to room temperature at a rate of 5 °C/h, yellowish bar-shaped crystals of **1**·α were obtained in a 30.1% yield. Anal. Calcd for $C_{10}H_{14}CdN_4O_{12}$ (**1**·α): C, 24.28; H, 2.85; N, 11.33. Found: C, 24.04; H, 2.68; N, 11.41. IR data (KBr, cm^{-1}): 3453s, 2922m, 2848m, 2663w, 2031w, 1576s, 1554s, 1419s, 1386s, 1313m, 1239m, 1106m, 1008m, 1027m, 974m, 867m, 834m, 801m, 782m, 655m, 531m, 455m.

$[Cd(H_2dcbi)_2(H_2O)_2]\cdot 2H_2O$ (1·*β* and 1·*γ*). A mixture of $CdSO_4\cdot {}^8/_3H_2O$ (0.066 g, 0.26 mmol), H_3dcbi (0.064 g, 0.40 mmol), oxalic acid (0.040 g, 0.30 mmol), 30% hydrogen peroxide (2 drops), and deionized water (7 mL) was stirred, and then it was transferred to and sealed in a 15 mL Teflon-lined bomb, which was heated to 150 °C for 90 h. After the mixture was cooled to room temperature at a rate of 5 °C/h, mixed yellowish crystals of **1**·*β* and **1**·*γ* were recovered in a 54% yield. Because X-ray powder diffraction patterns of **1**·*β* and **1**·*γ* simulated by single-crystal structural data are quite similar, the relative yield of **1**·*β* and **1**·*γ* and the purity of their bulk product could not be determined. Anal. Calcd for **1**·*β* $C_{10}H_{14}CdN_4O_{12}$: C, 24.28; H, 2.85; N, 11.33. Found: C, 24.10; H, 2.64; N, 11.39. IR data (KBr, cm^{-1}): 3433s, 3143s, 2431w, 1685s, 1653s, 1614s, 1399s, 1161s, 1081s, 947m, 867m, 526s. Anal. Calcd for **1**·*γ* $C_{10}H_{14}CdN_4O_{12}$: C, 24.28; H, 2.85; N, 11.33. Found: C, 24.14; H, 2.68; N, 11.40. IR data (KBr, cm^{-1}): 3424s, 3114s, 2435w, 1682s, 1609s, 1387s, 1151m, 1062m, 944m, 870m, 531s.

[Cd(Hdcbi)(H$_2$O)$_2$] (2). A mixture of $CdSO_4\cdot {}^8/_3H_2O$ (0.185 g, 0.72 mmol), H_3dcbi (0.078 g, 0.50 mmol), and deionized water (8 mL) was adjusted to pH ca. 6 with 3 M sodium hydroxide and transferred into a Teflon-lined bomb, which was heated to 145 °C for 5 days. After the mixture was cooled to room temperature at a rate of 5 °C per hour, yellow crystals were recovered in a 16% yield. Anal. Calcd for **2** $C_5H_6CdN_2O_6$: C, 19.85; H, 2.00; N, 9.26. Found: C, 19.63; H, 2.15; N, 9.08. IR data (KBr, cm^{-1}): 3442s,

(6) (a) Humphrey, S. M.; Wood, P. T. *J. Am. Chem. Soc.* **2004**, *126*, 13236. (b) Ciurtin, D. M.; Smith, M. D.; zur Loye, H. C. *Chem. Commun.* **2002**, 74. (c) Ciurtin, D. M.; Smith, M. D.; zur Loye, H. C. *Dalton Trans.* **2003**, 1245. (d) Tong, M. L.; Chen, X. M.; Batten, S. R. *J. Am. Chem. Soc.* **2003**, *125*, 16170. (e) Ghosh, S. K.; Bharadwaj, P. K. *Inorg. Chem.* **2005**, *44*, 3156. (f) Eubank, J. F.; Walsh, R. D.; Eddaoudi, M. *Chem. Commun.* **2005**, 2095.

(7) (a) Zhang, X. M.; Tong, M. L.; Chen, X. M. *Angew. Chem., Int. Ed.* **2002**, *41*, 1029. (b) Zhang, M. B.; Zhang, J.; Zheng, S. T.; Yang, G. Y. *Angew. Chem., Int. Ed.* **2005**, *44*, 1385. (c) Lu, J. Y. *Coord. Chem. Rev.* **2003**, *246*, 327.

(8) (a) Pan, L.; Huang, X.; Li, J.; Wu, Y.; Zheng, N. *Angew. Chem., Int. Ed.* **2000**, *39*, 527. (b) Pan, L.; Frydel, T.; Sander, M. B.; Huang, X.; Li, J. *Inorg. Chem.* **2001**, *40*, 1271.

(9) (a) Caudle, M. T.; Kampf, J. W.; Kirk, M. L.; Rasmussen, P. G.; Pecoraro, V. L. *J. Am. Chem. Soc.* **1997**, *119*, 9297. (b) Rajendiran, T. M.; Kirk, M. L.; Setyawati, I. A.; Caudle, M. T.; Kampf, J. W.; Pecoraro, V. L. *Chem. Commun.* **2003**, 824. (c) Bayon, J. C.; Net, G.; Ramussen, P. G.; Kolowich, J. B. *J. Chem. Soc., Dalton Trans.* **1987**, 3003. (d) Net, G.; Bayon, J. C.; Butler, W. M.; Ramussen, P. G. *Chem. Commun.* **1989**, 1022. (e) Angaridis, P.; Kampf, J. W.; Pecoraro, V. L. *Inorg. Chem.* **2005**, *44*, 3626. (f) Plieger, P. G.; Ehler, D. S.; Duran, B. L.; Taylor, T. P.; John, K. D.; Keizer, T. S.; McCleskey, T. M.; Burrell, A. K.; Kampf, J. W.; Haase, T.; Rasmussen, P. G.; Karr, J. *Inorg. Chem.* **2005**, *44*, 5761. (g) Maji, T. K.; Mostafa, G.; Chang, H.-C.; Kitagawa, S. *Chem. Commun.* **2005**, 2436. (h) Sun, Y.-Q.; Zhang, J.; Chen, Y.-M.; Yang, G.-Y. *Angew. Chem., Int. Ed.* **2005**, *44*, 5814.

Table 1. Crystallographic Data for Compounds **1**−**5**

	1·α	**1·β**	**1·γ**	**2**
formula	$C_{10}H_{14}CdN_4O_{12}$	$C_{10}H_{14}CdN_4O_{12}$	$C_{10}H_{14}CdN_4O_{12}$	$C_5H_6CdN_2O_6$
fw	494.65	494.65	494.65	302.53
temp (K)	298(2)	298(2)	298(2)	298(2)
cryst syst	monoclinic	monoclinic	monoclinic	orthorhombic
space group	$P2_1/c$	$C2$	$P2_1/n$	$Pbcn$
a (Å)	6.9069(13)	12.736(3)	10.947(9)	10.3466(6)
b (Å)	17.451(3)	7.0278(16)	6.991(6)	13.2179(8)
c (Å)	13.877(3)	10.939(2)	11.497(10)	13.1499(8)
α (deg)	90	90	90	90
β (deg)	97.639(3)	122.334(3)	111.153(15)	90
γ (deg)	90	90	90	90
V (Å^3)	1657.8(5)	827.3(3)	820.6(12)	1798.38(19)
Z	4	2	2	8
ρ (Mg/m^3)	1.982	1.986	2.002	2.235
μ (mm^{-1})	1.393	1.395	1.407	2.436
F(000)	984	492	472	1168
reflns independent	8049/3585	3061/1145	3306/1715	9569/1955
T_{max}/T_{min}	0.8967/0.6800	0.9335/0.7396	0.9330/7379	0.6163/0.5700
data/params	3585/0/244	1145/80/123	1715/0/124	1955/0/128
S params	0.965	1.126	1.083	1.047
R1[a]	0.0489	0.0809	0.0579	0.0255
wR2[b]	0.285	0.2275	0.1724	0.0726
$\Delta\rho_{max}/\Delta\rho_{min}$	2.275/−0.781	4.930/−0.998	1.201/−0.920	0.971/−0.436

	3	**4**	**5**	**6**	**7**
formula	$C_5H_4CdN_2O_5$	$C_{20}H_{14}Cd_5N_8O_{20}$	$C_7H_2Cd_2N_2O_8$	$C_{11}H_4Ag_5N_5O_8$	$C_5H_4MnN_2O_5$
fw	284.50	1248.39	466.91	873.54	227.04
temp (K)	298(2)	298(2)	298(2)	298(2)	298(2)
cryst syst	orthorhombic	orthorhombic	monoclinic	monoclinic	orthorhombic
space group	$Pbca$	$Pnma$	$C2/m$	$P2_1/c$	$Pbca$
a (Å)	7.1581(9)	14.268(3)	11.549(7)	17.495(13)	7.213(2)
b (Å)	13.6854(18)	16.017(4)	16.579(13)	6.862(8)	13.614(4)
c (Å)	14.7668(19)	15.721(3)	7.317(4)	13.081(17)	14.255(4)
α (deg)	90	90	90	90	90
β (deg)	90	90	129.171(10)	97.37(12)	90
γ (deg)	90	90	90	90	90
V (Å^3)	1446.6(3)	3592.6(14)	1086.2(13)	1557(3)	1399.8(7)
Z	8	4	4	4	8
ρ (Mg/m^3)	2.613	2.308	2.855	3.726	2.155
μ (mm^{-1})	3.009	3.000	3.955	6.238	1.876
F(000)	1088	2360	872	1616	904
reflns independent	6548/1576	21401/2689	2579/1222	12880/3702	6324/1530
T_{max}/T_{min}	0.5844/0.4862	0.8645/0.4980	0.6931/0.4380	0.5215/0.3046	0.8062/0.8493
data/params	1576/0/119	2689/6/241	1222/0/92	3702/0/262	1530/0/118
S params	1.088	1.065	1.102	1.053	0.929
R1[a]	0.0265	0.0498	0.0236	0.0288	0.0446, 0.0695
wR2[b]	0.0582	0.1455	0.0649	0.0693	0.0746, 0.0789
$\Delta\rho_{max}/\Delta\rho_{min}$	0.816/−1.326	4.747/−2.540	0.869/−0.984	1.875/−1.901	0.491/−0.507

[a] $R1 = \sum||F_o| - |F_c||/\sum|F_o|$. [b] $wR2 = [\sum[w(F_o^2 - F_c^2)^2]/\sum[w(F_o^2)^2]]^{1/2}$.

2926w, 2833w, 1654m, 1588s, 1376m, 1296w, 1217w, 1164m, 1071s, 992m, 939w, 634m, 514m, 422w.

[Cd(Hdcbi)(H$_2$O)] (3). A mixture of $CdCl_2 \cdot 2.5H_2O$(0.034 g, 0.15 mmol) and H_3dcbi (0.046 g, 0.30 mmol) in a molar ratio of 1:2 was dissolved in deionized water (4 mL) and stirred for 20 min in air; MeCN (3 mL) was added to the mixture. The solution was transferred into a 15 mL Teflon-lined stainless steel bomb and heated at 140 °C for 4 days. After the mixture was cooled to room temperature at a rate of 5 °C/h, yellowish block crystals were collected in ca. 53.6% yield. Anal: calc. for **3** $C_5H_4CdN_2O_5$: C, 21.11; H, 1.42; N, 9.85. Found: C, 21.34; H, 2.16; N, 8.95. IR data (KBr, cm^{-1}): 3409s, 3129w, 3055w, 2966w, 2863m, 2656w, 1591s, 1557s, 1495s, 1456s, 1377s, 1326m, 1241s, 1168w, 1077m, 974w, 920w, 870m, 797s, 664s, 516s.

[Cd$_5$(Hdcbi)$_2$(dcbi)$_2$(H$_2$O)]·*x*H$_2$O (*x* ≈ 6) (4). A mixture of $CdCl_2 \cdot 2.5H_2O$(0.114 g, 0.50 mmol) and H_3dcbi (0.046 g, 0.30 mmol) in a molar ratio of 5:3 was dissolved in 3 mL of MeCN and 4 mL of water under stirring at room temperature. The resulting solution was transferred into Teflon-lined bomb and heated at 145 °C for 5 days. After the mixture was cooled to room temperature at a rate of 5 °C/h, yellow crystals were obtained in a 50.5% yield. Anal. Calcd for (**4**) $C_{20}H_{20}Cd_5N_8O_{23}$: C, 18.44; H, 1.55; N, 8.60. Found: C, 18.23; H, 1.61; N, 8.52. IR data (KBr, cm^{-1}): 3439s, 2923w, 2844w, 1575s, 1484s, 1386s, 1298w, 1254m, 1106m, 1003w, 870w, 826w, 782w, 664m, 531w.

[Cd$_2$(Hdcbi)(C$_2$O$_4$)] (5). A mixture of $CdSO_4 \cdot {}^8/_3H_2O$ (0.127 g, 0.50 mmol), H_3dcbi (0.064 g, 0.40 mmol), oxalic acid (0.040 g, 0.30 mmol), and hydrogen peroxide (6 drops, 30%) was dissolved in 7 mL of water under stirring at room temperature. The solution then was transferred into Teflon-lined bomb and heated at 170 °C for 60 h. Pale yellow block crystals were obtained in a 58% yield after the mixture was cooled to room temperature at a rate of 5 °C/h. Anal. Calcd for $C_7H_2Cd_2N_2O_8$ **(5)**: C, 18.01; H, H, 0.43; N, 6.00. Found: C, 18.16; H, H 0.45; N, 5.93. IR data (KBr, cm^{-1}): 3424m, 2939w, 2844w, 1679s, 1614s, 1486s, 1431m, 1407m, 1320s, 1256m, 1121m, 1010w, 875w, 769s, 653s, 518m, 446w.

[Ag$_5$(Hdcbi)$_2$(CN)] (6). A mixture of $AgNO_3$ (0.105 g, 0.60 mmol) and H_3dcbi (0.039 g, 0.25 mmol) was dissolved in 3 mL of

Table 2. Selected Bond Lengths (Å) for **1**−**7**[a]

		1·α	
Cd(1)−O(1W)	2.251(4)	Cd(1)−O(2W)	2.285(4)
Cd(1)−N(1)	2.264(4)	Cd(1)−O(3W)	2.380(4)
Cd(1)−N(3)	2.264(4)		
		1·β	
Cd(1)−O(3)	2.20(2)	Cd(1)−O(1W)	2.325(10)
Cd(1)−O(3a)	2.20(2)	Cd(1)−N(2a)	2.37(2)
Cd(1)−O(1Wa)	2.325(10)	Cd(1)−N(2)	2.37(2)
		1·γ	
Cd(1)−N(2a)	2.272(5)	Cd(1)−O(1W)	2.327(6)
Cd(1)−N(2)	2.272(5)	Cd(1)−O(3)	2.341(5)
Cd(1)−O(1Wa)	2.327(6)	Cd(1)−O(3a)	2.341(5)
		2	
Cd(1)−N(1a)	2.226(2)	Cd(1)−O(2W)	2.359(2)
Cd(1)−N(2)	2.237(3)	Cd(1)−O(3)	2.378(2)
Cd(1)−O(1W)	2.330(3)	Cd(1)−O(1a)	2.418(2)
		3	
Cd(1)−O(1W)	2.234(2)	Cd(1)−O(4b)	2.302(2)
Cd(1)−N(2a)	2.266(2)	Cd(1)−O(1a)	2.316(2)
Cd(1)−O(3)	2.271(2)	Cd(1)−O(2b)	2.394(2)
		4	
Cd(1)−N(2b)	2.238(7)	Cd(2)−O(4b)	2.338(7)
Cd(1)−O(8c)	2.246(8)	Cd(2)−O(5d)	2.442(7)
Cd(1)−N(4)	2.246(7)	Cd(2)−O(1)	2.472(7)
Cd(1)−O(1)	2.293(6)	Cd(3)−O(1W)	2.32(3)
Cd(1)−O(8)	2.458(7)	Cd(3)−O(7e)	2.180(9)
Cd(1)−O(4b)	2.580(7)	Cd(3)−O(7c)	2.180(9)
Cd(2)−O(5)	2.240(7)	Cd(3)−O(6)	2.199(8)
Cd(2)−N(3d)	2.259(8)	Cd(3)−O(6a)	2.199(8)
Cd(2)−N(1)	2.265(8)		
		5	
Cd(1)−N(1a)	2.225(3)	Cd(1)−O(3)	2.421(2)
Cd(1)−O(1)	2.249(3)	Cd(1)−O(4a)	2.427(3)
Cd(1)−O(4b)	2.326(3)	Cd(1)−O(1a)	2.465(3)
Cd(1)−O(3c)	2.339(2)		
		6	
Ag(1)−N(4e)	2.100(4)	Ag(3)−O(7d)	2.309(4)
Ag(1)−N(1)	2.104(4)	Ag(3)−Ag(1)	3.229(3)
Ag(1)−Ag(2)	3.143(3)	Ag(4)−C(11a)	2.090(4)
Ag(2)−O(6)	2.285(4)	Ag(4)−N(2b)	2.139(4)
Ag(2)−O(1f)	2.288(4)	Ag(4)−Ag(3)	2.829(4)
Ag(2)−N(5g)	2.340(4)	Ag(5)−N(5)	2.125(4)
Ag(3)−C(11a)	2.210(5)	Ag(5)−N(3)	2.130(4)
Ag(3)−O(3c)	2.242(4)		
		7	
Mn(1)−O(1W)	2.144(3)	Mn(1)−O(4b)	2.198(3)
Mn(1)−O(1)	2.170(3)	Mn(1)−N(2b)	2.226(3)
Mn(1)−O(2a)	2.172(3)	Mn(1)−O(3a)	2.258(3)

[a] Symmetry codes for **1·β**: a $-x, y, -z+2$. For **1·γ**: a $-x, -y, -z+2$. For **2**: a $-x+1/2, y+1/2, z$. For **3**: a $-x+1/2, -y+1, z-1/2$; b $-x, -y+1, -z+1$. For **4**: a $x, -y+1/2, z$; b $-x+1/2, -y+1, z+1/2$; c $-x, -y+1, -z+2$; d $-x+1, -y+1, -z+2$; e $-x, y-1/2, -z+2$. For **5**: a $-x+1/2, -y+1/2, -z+1$; b $x-1/2, -y+1/2, z$; c $-x, y, -z$. For **6**: a $x, -y-1/2, z+1/2$; b $-x+1, y-1/2, -z+1/2$; c $-x+1, -y, -z+1$; d $-x, y-1/2, -z+1/2$; e $-x, -y, -z$; f $x, -y+1/2, z-1/2$; g $x, -y+1/2, z+1/2$. For **7**: a $-x+2, -y, -z+1$; b $-x+3/2, -y, z+1/2$.

acetonitrile and 2 mL of water under stirring at room temperature. The solution then was transferred into Teflon-lined bomb and heated at 150 °C for 72 h. Colorless block crystals were obtained in a 62% yield after the mixture was cooled to room temperature at a rate of 5 °C/h. Anal. Calcd for **6** $C_{11}H_4Ag_5N_5O_8$: C, 15.12; H, 0.46; N, 8.02. Found: C, 14.94; H, 0.67; N, 7.88. IR data (KBr, cm^{-1}): 3427s, 3407s, 2446m, 2371m, 2064m, 1685s, 1657s, 1609s, 1458m, 1397s, 1267m, 1129s, 1608s, 992m, 951s, 869s, 821m, 759w, 622m, 567m, 540s, 512s.

[Mn(Hdcbi)(H_2O)] (7). Compound **7** was synthesized by a procedure similar to that for **3** (46% yield). Anal. Calcd for **7** $C_5H_4MnN_2O_5$: C, 26.45; H, 1.78; N, 12.34. Found: C, 26.14; H, 1.86; N, 12.08.

Crystallographic Studies. X-ray single-crystal diffraction data were collected on a Bruker SMART APEX CCD diffractometer at 298(2) K using Mo Kα radiation ($\lambda = 0.71073$ Å). The program SAINT was used for integration of the diffraction profiles. All the structures were solved by direct methods using the SHELXS program of the SHELXTL package and refined by the full-matrix least-squares methods with SHELXL.[10] The hydrogen atoms of the ligands were generated theoretically onto the specific atoms and refined isotropically with fixed thermal factors. The solvent water molecules in **4** could not be localized from the Fourier map but were deduced by elemental analysis and TGA. Further details for structural analyses and selected bond lengths are summarized in Tables 1 and 2, respectively.

Results and Discussions

IR Spectra. The strong and broad absorption bands in the range of 3400−3500 cm^{-1} in **1**, **2**, **3**, and **4** indicate the presence of hydrogen-bonded water molecules, while the absence of bands in this range is suggestive of the absence of coordinated and lattice water molecules. The strong bands of the N−H stretching frequencies in **1·α**, **1·β**, **1·γ**, and **3** are covered by the broad absorption band of hydrogen-bonded water molecules. In addition, the uncoordinate carboxylate group in **1·α** is indicated by the the $\nu_{asym}(CO_2)$ band at 1554 and the $\nu_{sym}(CO_2)$ band at 1419 cm^{-1} giving a $\Delta\nu$ value 135 cm^{-1}. The coordination of the carboxylate can be seen from the strong bands in the range of 1350−1700 cm^{-1} in **1·β**, **1·γ**, **2**, **3**, **4**, **5**, and **6.** In complexes **1·β**, **1·γ**, **2**, and **6**, the unidentate mode of binding (Scheme 1a−c and i) shows two very strong broad ν_{asym} and ν_{asym} stretching bands in the region of 1550−1610 and 1300−1420 cm^{-1}, respectively, with a $\Delta\nu$ value of 190−230 cm^{-1}. For the bidentate chelate coordination mode (Scheme 1g and l) in **3** and **4**, the $\nu_{sym}(CO_2)$ band occurs at a lower frequency at 1420−1500 cm^{-1} giving a $\Delta\nu$ value of 90−100 cm^{-1}. For complex **5**, no differences between the unidentate-binding Hdcbi group (Scheme 1h) and the multidentate oxalate could be extracted from the $\nu_{asym}(CO_2)$ and $\nu_{asym}(CO_2)$ stretching frequencies or $\Delta\nu$ values. The strong bands in the range of 1590−1680 cm^{-1} in all these complexes imply the C═N and C═C stetching bands of imidazole ring in H_3dcbi. The presence of cyanide in **6** is indicated by a band at 2064 cm^{-1}.

Crystal Structure. Complex **1** has three polymorphs (**1·α**, **1·β**, and **1·γ**), and they all show a neutral mononuclear structure, as shown in Figure 1. The asymmetric unit of **1·α** consists of one crystallographically independent Cd(II), two singly deprotonated H_2dcbi groups, and three coordinated water molecules. The Cd(II) ion shows trigonal bipyramidal geometry, coordinated by two nitrogen atoms from two H_2dcbi groups and three water molecules. The asymmetric units in **1·β** and **1·γ** consist of one crystallographically independent Cd(II), one H_2dcbi group, one coordinated water molecule, and one lattice water molecule. The Cd(II) in **1·β**

(10) Sheldrick, G. M. *SHELXTL, Crystallographic Software Package*, version 5.1; Bruker-AXS: Madison, WI, 1998.

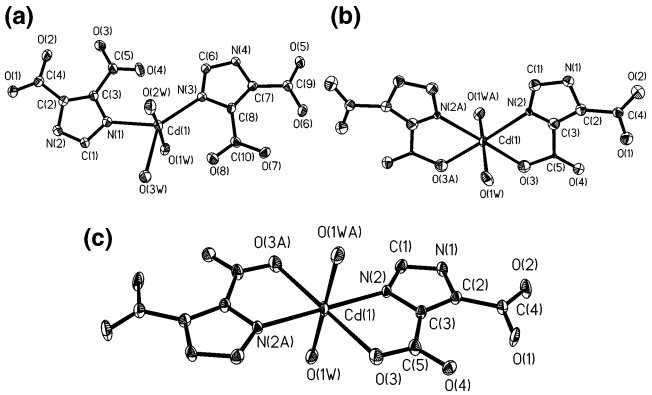

Figure 1. View of the structure of **1**·α (a), **1**·β (b), and **1**·γ (c) with 35% thermal ellipsoids.

localizes on the C_2 axis and shows a distorted octahedral geometry. The Cd(II) in **1**·γ localizes at an inversion center and also shows a distorted octahedral geometry. The Cd−N and Cd−O distances in the three polymorphs are in the range of 2.264(4)−2.360(19) Å and 2.20(2)−2.380(4) Å. The singly deprotonated H_2dcbi in **1**·α is coordinated to the Cd(II) in a monodentate mode via the imidazole-N atom (Scheme 1a), while in **1**·β and **1**·γ, H_2dcbi is coordinated to Cd(II) in a N,O-chelating mode (Scheme 1b) that is observed in $[Mn(H_2dcbi)_2(H_2O)_2]$ and $[Cd(H_2dcbi)_2(H_2O)_2]$.[11]

The local geometry of $[Cd(H_2dcbi)_2(H_2O)_2]$ in **1**·β and **1**·γ is different, and the former belongs to the C_2 point group, while the latter belongs to the C_i point group. **1**·β and **1**·γ are cis and trans geometrical isomers, while **1**·α is their hydrated isomer. There are O−H···O and N−H···O hydrogen bonds among the carboxyl-O, imidazole-N, and water molecules, which extend discrete molecules of **1** into a three-dimensional supramolecular array (Figure S1). It is worth noting that **1**·β and **1**·γ have similar three-dimensional supramolecular arrays, resulting in similar simulated X-ray powder diffraction patterns for **1**·β and **1**·γ (Figure S2).

Complex **2** crystallizes in the orthorhombic space group *Pbcn* and the asymmetric unit consists of one Cd(II), one doubly deprotonated Hdcbi and two water molecules. The Cd(II) ion has a distorted octahedral geometry, being chelated by N and O atoms in the equatorial plane to form two stable five-membered rings, as shown in Figure 2. The two axial sites are occupied by water molecules. The Cd(1)−L (L = O, N) distances are in the range of 2.226(3)−2.418(2) Å and the trans L−Cd−L bond angles are in the range of 153.38(11)−163.79(8)°. The bis-N,O-chelating μ_2 coordination mode of Hdcbi is shown in Scheme 1d, which is the same as that in $\{[Fe(3,5\text{-}Bu_2\text{-salpn})]_2(Hdcbi)\}$.[9e] The connections of the Cd(II) atoms by Hdcbi form the one-dimensional chainlike structure of **2**.

The asymmetric unit in **3** consists of one Cd(II), one doubly deprotonated Hdcbi, and one water molecule. Cd(II) shows a distorted octahedral environment, coordinated by three Hdcbi groups and one water molecule, as shown in Figure 3. Among the three Hdcbi groups, one chelates Cd(II)

(11) (a) Zhang, X. M.; Fang, R. Q.; Wu, H. S.; Ng, S. W. *Acta Crystallogr. E* **2004**, *60*, m12. (b) Ma, C.; Chen, F.; Chen, C.; Liu, Q. *Acta Crystallogr. C* **2003**, *59*, m516.

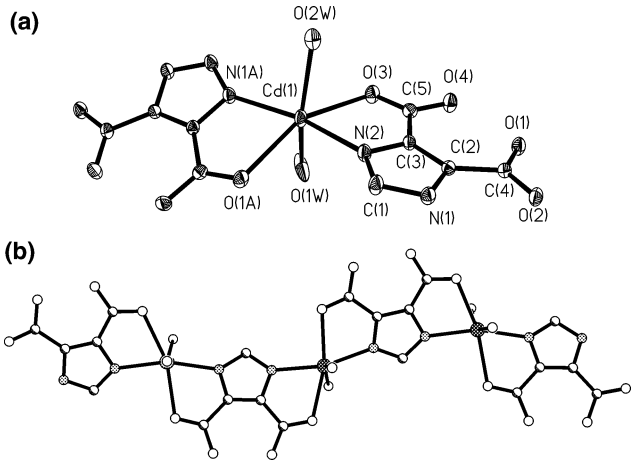

Figure 2. View of the coordination environment of cadmium with 35% thermal ellipsoids (a) and of the 1-D chain (b) in **2**.

in a N,O-mode to form a five-membered ring; the second Hdcbi chelates the Cd(II) ion in an O,O′-mode to form a seven-membered ring, while the third Hdcbi binds Cd(II) in a monodentate mode via one carboxylate oxygen. The Cd(1)−L (L = O, N) distances are in the range of 2.234(2)−2.394(2) Å and the trans L−Cd−L bond angles are in the range of 151.51(7)−167.79(8)°. It is worth noting that Hdcbi in **3** adopts a new μ_3-*k*N,O:*k*O′:*k*O″,O‴ coordination mode (Scheme 1g) to bridge three Cd(II) atoms in N,O-chelating, O,O′-chelating, and monodentate fashions. The overall structure of **3** is a two-dimensional wavelike (4,4) topological layer, as illustrated in Figure 3b, in which four-connected nodes and two-connected connectors are provided by dicadmium units and Hdcbi groups, respectively. The two-dimensional (4,4) topological layer of **3** is similar to the structural motif of $[Cd_2(pdc)_2(H_2O)_2]$ in compound $[Cd_3(pdc)_2(H_2O)_2]$.[8b] The 2-D layers are stacked in an AA fashion along the *a* axis with an interlayer separation of ca. 7.16 Å (Figure S3).

Compound **4** crystallizes in orthorhombic space group *Pnma*, and the asymmetric unit consists of three crystallographically independent Cd(II) ions, one doubly deprotonated Hdcbi, two half triply deprotonated dcbi, and three water molecules, as shown in Figure 4. Both Cd(1) and Cd(2) display distorted octahedral geometries, each coordinated by four Hdcbi molecules via monodentate and N,O-chelating modes. The Cd−L (L = O, N) distances are in the range of 2.238(7)−2.580(8) Å. The trans L−Cd−L bond angles for Cd(1) and Cd(2) are in the range of 131.5(3)−164.6(2) and 133.3(3)−145.1(3)°, respectively, indicating highly distorted octahedra. Cd(3) shows a square-pyramidal geometry, coordinated by two dcbi groups in the O,O′-mode within the equatorial plane and one water molecule at the apical site. The Cd(3)−O distances in the equatorial plane are 2.180(9) and 2.199(8) Å, which are a little shorter than average Cd−O distance. The cis L−Cd(3)−L bond angles are in the range of 87.8(5)−93.6(4)°. Interestingly, doubly deprotonated Hdcbi and triply deprotonated dcbi coexist in **4**, and they adopt two new types of coordination modes, namely, μ_4-*k*N,O:*k*O:kN′,O′:*k*O′ (Scheme 1h) and μ_5-*k*N,O:*k*O:kN′,O′:*k*O′:*k*O″,O‴ (Scheme 1l). Along the *a* axis, the $Cd(1)O_4N_2$

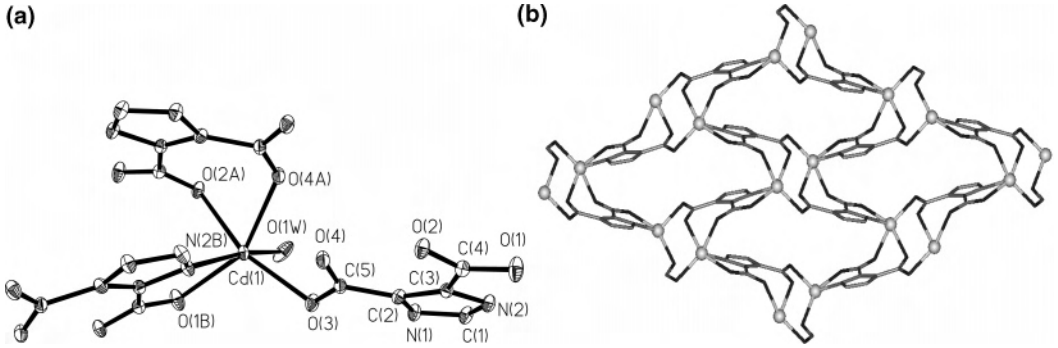

Figure 3. View of the coordination environment of cadmium with 35% thermal ellipsoids (a) and the 2-D layer along the *b* axis (b) in **3**.

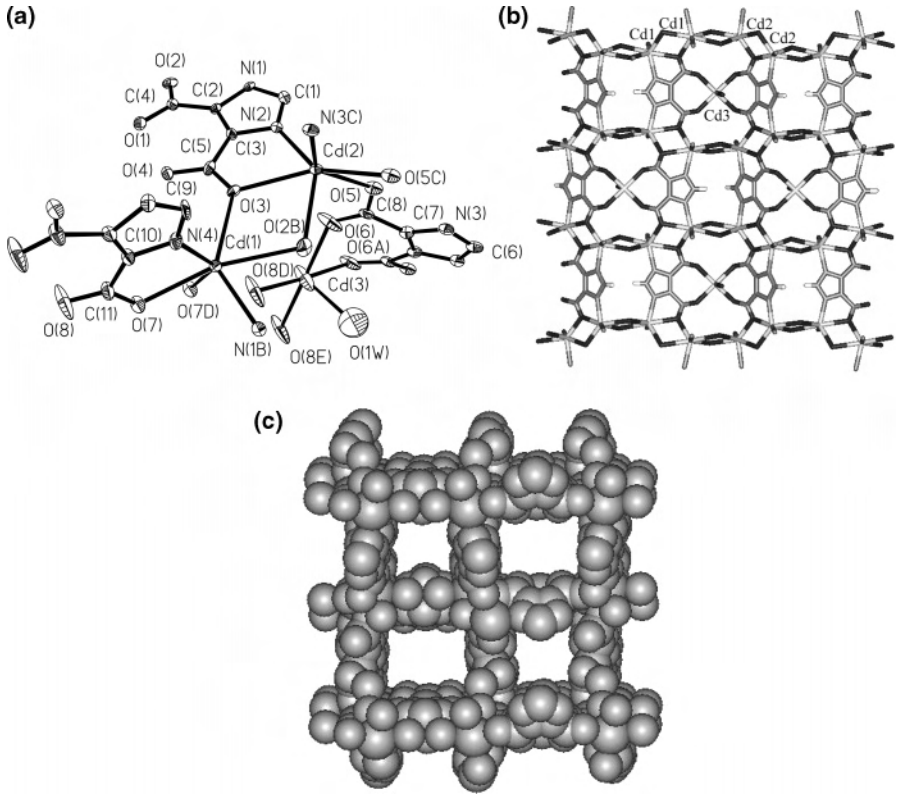

Figure 4. View of the coordination environments of cadmium atoms with 35% thermal ellipsoids (a), the 2-D motif along the *b* axis (b), and the 3-D framework with 1-D channels (c) in **4**.

and $Cd(2)O_4N_2$ octahedra are linked via edge-sharing into an inorganic chain with a repeat sequence of Cd(1)−Cd(1)−Cd(2)−Cd(2), and the inorganic chains are connected in a cross fashion by Hdcbi and dcbi into a three-dimensional framework. Such a three-dimensional framework has available sites, each of which is enclosed by four carboxylate oxygen atoms from two face-to-face dcbi groups (Figure 4b). In fact, these available sites are occupied by Cd(3) atoms via coordination to finish the three-dimensional coordination framework with one-dimensional channels that are occupied by solvent water molecules (Figure 4c). After the van der waals radii of the surface atoms were removed, the free channel is sized ca. 4 × 7 Å. A calculation by *PALTON*[12] indicates the free volume of channels occupy 16.3% of the crystal volume.

(12) Spek, A. L. *PLATON, A Multipurpose Crystallographic Tool*; Untrecht University: Utrecht, The Netherlands, 1999.

Compound **5** crystallizes in monoclinic space group *C*2/*m*, and the asymmetric unit consists of crystallographically independent one Cd(II), half doubly deprotonated Hdcbi and half oxalate as shown in Figure 5. The crystallographic 2-fold axis passes through the C(2) atom and bisects the Hdcbi group. The seven-coordinate Cd(II) site shows a coordination geometry close to pentagonal bipyramid and is chelated by Hdcbi in the N,O-mode and oxalate in the O,O′-mode. The additional three coordination sites are occupied by three monodentate oxygen atoms from two oxalates and one Hdcbi to finish the seven-coordinate geometry. The Cd−L (L = O, N) distances are in the range of 2.226(3)−2.466(3) Å. The coordination mode of the doubly deprotonated Hdcbi is μ_4-*k*N,O:*k*O:*k*N′,O′:*k*O′ as shown in Scheme 1h. It is worth noting that the oxalate in **5** shows an uncommon μ_6- mode, which results in a sheetlike $[Cd_2(ox)]_n^{2n+}$ structural motif within the [010] plane. The $[Cd_2(ox)]_n^{2n+}$ sheets are pillared

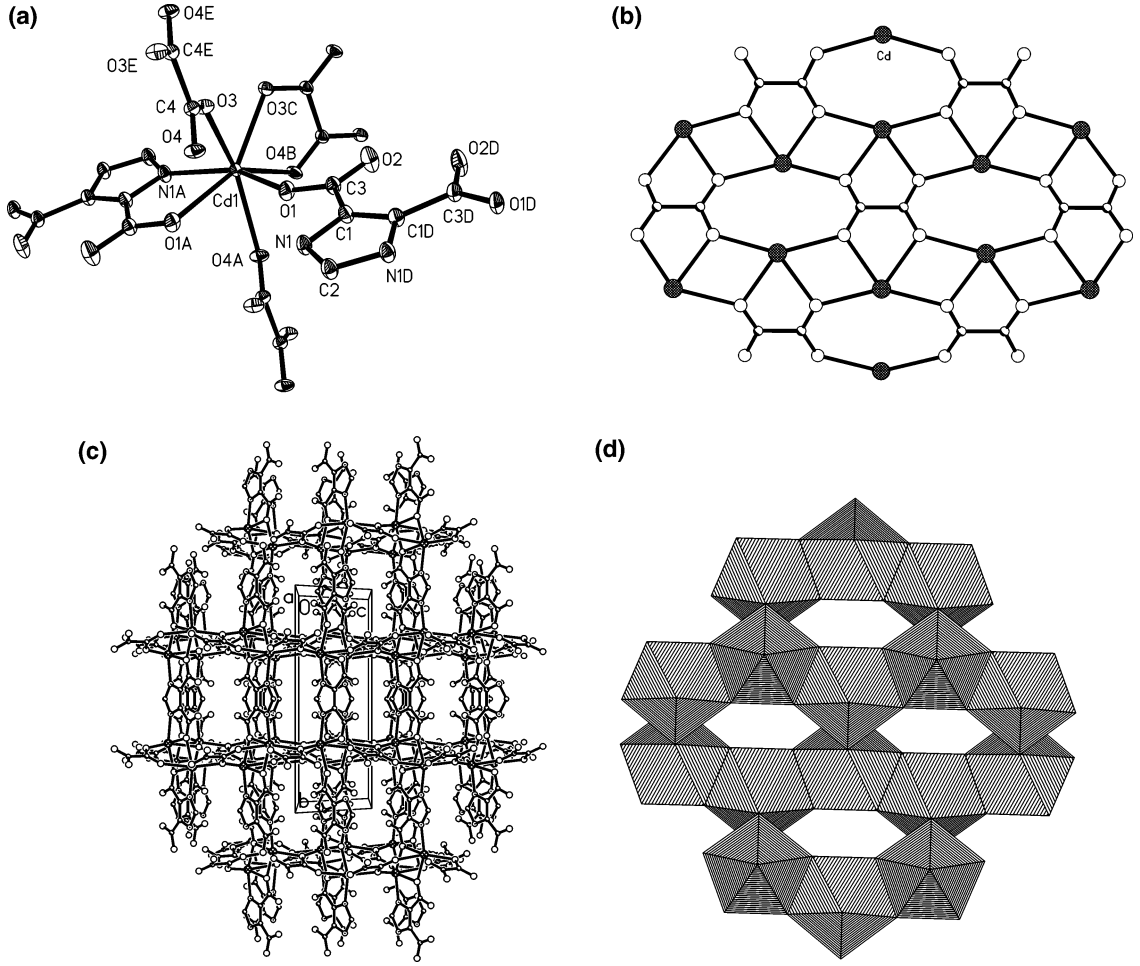

Figure 5. View of the coordination environment of the cadmium atom with 35% thermal ellipsoids (a), the sheetlike $[Cd_2(ox)]_n^{2n+}$ structural motif (b), the 3-D framework (c), and the Cd/O/N layer (d) in **5**.

by Hdcbi groups to generate a three-dimensional framework. One of unique features of **5** is presence of an inorganic Cd/O/N layer constructed by edge-sharing of $CdNO_6$ pentagonal bipyramids. To the best our knowledge, such an inorganic Cd/O/N layer has not been documented.

Compound **6** crystallizes in the monoclinic space group *Pnma*, and the asymmetric unit consists of five crystallographically independent Ag(I), two doubly deprotonated Hdcbi, and one cyanide as shown in Figure 6. All atoms localize in general positions. The presence of cyanide is confirmed by the C(11)−N(5) bond length of 1.135(6) Å and the IR absorption band at 2064 cm^{-1}.[13] The Ag(1), Ag(4), and Ag(5) atoms are two-coordinate, while Ag(2) and Ag(3) are three-coordinate. Ag(1) shows a close linear coordination geometry coordinated by two nitrogen atoms from two different Hdcbi groups with Ag(1)−N distances of 2.100(4) and 2.104(4) Å and an N−Ag(1)−N angle of 175.34(13)°; Ag(2) shows a close trigonal coordination geometry, coordinated by two oxygen atoms from two Hdcbi groups and one nitrogen atom of cyanide with Ag(2)−L (L = O, N) distances of 2.285(4)−2.340(4) Å and L−Ag(2)−L angles of 96.66(14)−124.21(15)°. Ag(3) shows a geometry between triangle and T-shaped, coordinated by two oxygen atoms and one nitrogen from three different Hdcbi groups with Ag(3)−L (L =O, N) distances of 2.210(5)−2.309(4) Å and L−Ag(3)−L angles of 83.76(14)−159.37(14)°, and Ag(4) shows a linear coordination geometry coordinated by one imidazole nitrogen and one carbon of cyanide with Ag(3)−L (L =C, N) 2.090(4) and 2.139(4) Å and an L−Ag(4)−L angle of 172.92(15) °; Ag(5) is coordinated by one imidazole nitrogen and one nitrogen of cyanide with Ag(5)−N distances of 2.125(4) and 2.130(4) Å and an L−Ag(5)−L angle of 172.07(14)°. Interestingly, the doubly deprotonated Hdcbi adopts an unprecedented μ_4-*k*N:*k*O:*k*N′:*k*O′ coordination (Scheme 1i). It is quite unusual for Hdcbi to adopt such a coordination mode because it does not form a stable five-membered ring. The presence of μ_4-*k*N:*k*O:*k*N′:*k*O′ Hdcbi is possibly caused by the nature of the Ag(I) ions, such as the lower coordination number and softer acidity than that of the Cd(II) ion. The cyanide adopts a rare μ_4-*k*C,*k*C:*k*N,*k*N mode, which is only observed in several double, triple, and quadruple silver salts.[13] In addition, it should be noted that there are short Ag···Ag distances [Ag(1)−Ag(2) = 3.143(3) Å, Ag(3)−Ag(1) = 3.229(3) Å, and Ag(4)−Ag(3) = 2.829(4) Å] which are comparable to

(13) (a) Wang, Q.-M.; Mak, T. C. W. *J. Am. Chem. Soc.* **2001**, *123*, 1501. (b) Wang, Q.-M.; Mak, T. C. W. *Chem. Commun.* **2000**, 1435. (c) Guo, G.-C.; Mak, T. C. W. *Angew. Chem., Int. Ed. Engl.* **1998**, *37*, 3183.

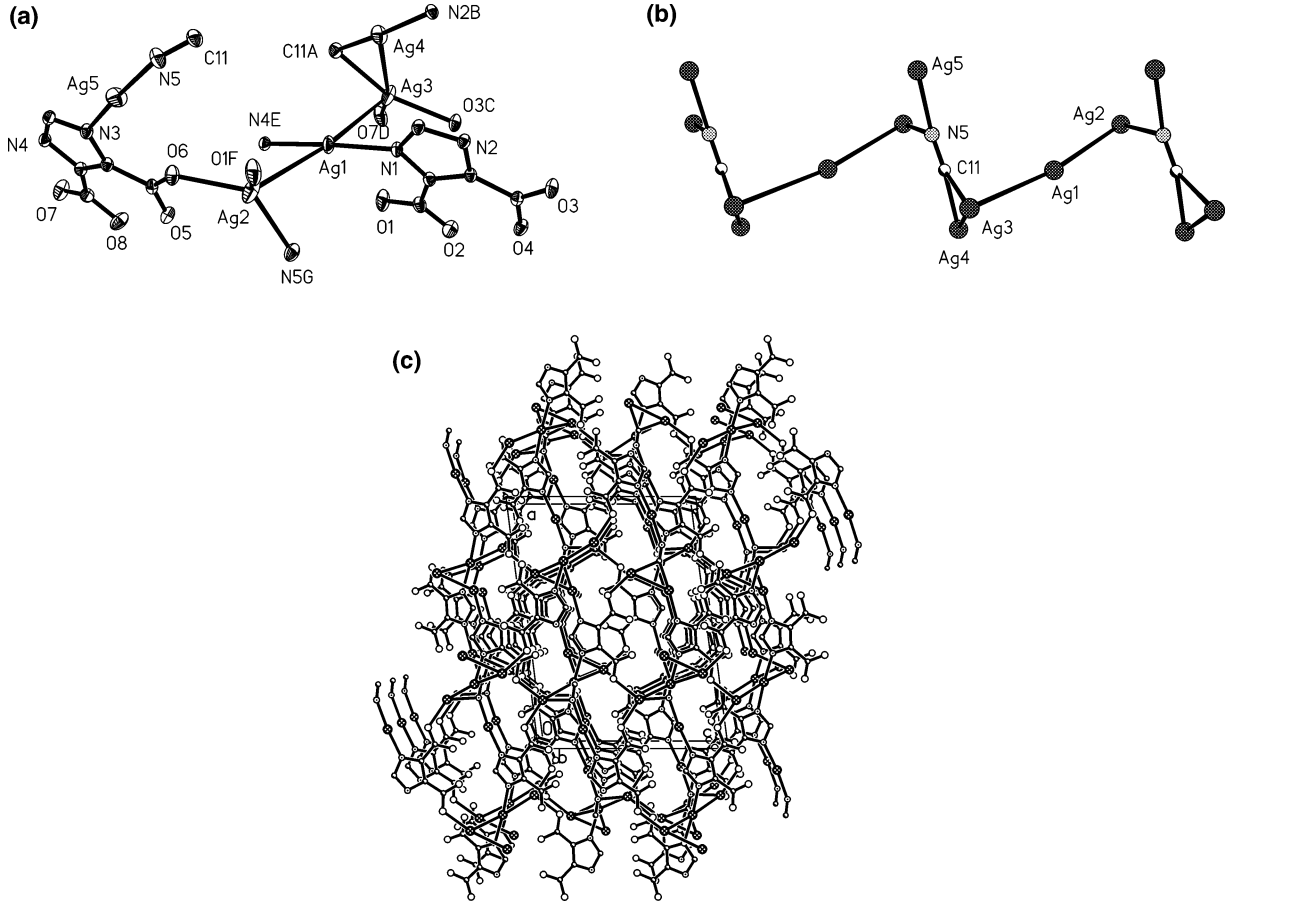

Figure 6. View of the coordination environments of the Ag(I) atoms with 35% thermal ellipsoids (a), the chainlike $[Ag_5(CN)]_n^{4n+}$ structural motif (b), and the 3-D framework (c) in **6**.

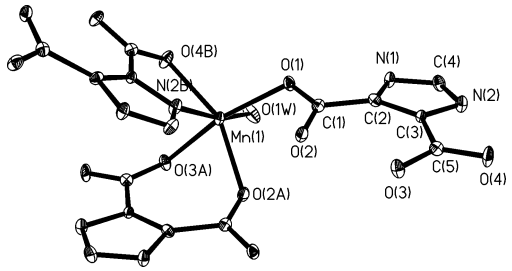

Figure 7. View of the coordination environment of the Mn(II) atom with 35% thermal ellipsoids in **7**.

the interatomic contact of 2.89 Å in metallic silver, indicating Ag(I)···Ag(I) interactions. The coordination of cyanide to the Ag(I) ions produces $[Ag_4CN]^{3+}$ units which are bridged by Ag(1) ions via Ag···Ag interactions into a $[Ag_5CN]_n^{4n+}$ chain. The $[Ag_5CN]_n^{4n+}$ chains are linked by Hdcbi into a complicated three-dimensional framework.

Compound **7** is isostructural with **3**, and Mn(II) shows a distorted octahedral environment similar to Cd(II) in **3**, coordinated by three Hdcbi groups and one water molecule, as shown in Figure 7. The Mn(1)−L (L = O, N) distances are in the range of 2.144(3)−2.258(3) Å, which are shorter than the Cd(1)−L distances in isostructural **3**. The overall structure of **7** is a two-dimensional wavelike (4,4) topological layer as illustrated in Figure 3b.

Synthesis Chemistry. The synthetic conditions, structural dimensions, and coordination modes of $H_n$dcbi for five cadmium complexes are tabulated in Table 3. The deprotonation process of free H_3dcbi has been discussed before,[14] which gives a suitable explanation to the diversity of the coordination modes. The strong internal bond between COOH and COO^- makes one carboxylic hydrogen atom more acidic, and thus this carboxylic hydrogen atom tends to be removed at a lower pH value of ca. 1.5. The second carboxylic hydrogen starts to be removed at a pH value ca. 3.2. The removal of imidazole-H seems to be more difficult than the two carboxylic hydrogen atoms. However, in the presence of transition metal ions, the removal of the three H_3dcbi hydrogen atoms is somewhat different from the free H_3dcbi. For example, the imidazole hydrogen can be removed by the stabilization of N−M−O−C−C five-membered chelate ring. The general deprotonation process

Table 3. Influences of Solvent and M/L Molar Ratio on Products and Coordination Modes of $H_n$dcbi

complex	dimension	Cd/L	solvent	*T* (°C)	duration	species	mode
1·α	0-D	2:3	H_2O	140	4	H_2dcbi	1a
1·*β*, **1**·*γ*	0-D	2:3	H_2O	145	3.75	H_2dcbi	1b
2	1-D	7:5	H_2O	145	5	Hdcbi	1d
3	2-D	1:2	H_2O/MeCN	140	4	Hdcbi	1g
4	3-D	5:3	H_2O/MeCN	145	5	Hdcbi, dcbi	1h, 1l
5	3-D	5:4	H_2O/MeCN	170	2.5	Hdcbi	1h

(14) Sanna, D.; Micera, G.; Buglyo, P.; Kiss, T.; Gajda, T.; Surdy, P. *Inorg. Chim. Acta* **1998**, *268*, 297.

of H_3dcbi can be denoted as

$$H_3dcbi \overset{-H^+}{\rightleftharpoons} H_2cdbi^- \overset{-H^+}{\rightleftharpoons} Hdcbi^{2-} \overset{-H^+}{\rightleftharpoons} dcbi^{3-}$$

If Cd(II) ions are superfluous in the system, the chemical balance should right shift with the coordination of Cd(II) ions and ligands, but the increase of the proton concentration will counteract the right shift of the chemical balance. Thus the method of neutralization of the generated proton is a key to the triple deprotonation of H_3dcbi to form dcbi. As can be deduced, solvent MeCN is preferable to water in the formation of complexes of triply deprotonated dcbi ligand. The molar ratios of M/L in the syntheses of **2** and **4** are very close, and the reaction temperature and time are same. But replacement of solvent water by H_2O/MeCN resulted in a structural change from chainlike **2** to the 3-D framework of **4**. Also, species of $H_n$dcbi are accordingly changed from doubly deprotonated Hdcbi to a mixture of Hdcbi and dcbi.

If Cd(II) ions are insufficient, the M/L molar ratio is a very important factor to product. This trend is apparent in the synthesis of mononuclear **1** and 1-D chainlike **2**. Complexes **1** and **2** were obtained from an aqueous system, and the reaction temperature and time are also similar. But a lower M/L molar ratio (2:3) results in mononuclear **1** while a higher M/L molar ratio (3:2) forms chainlike **2**. In addition, both **3** and **4** were produced in the mixture of MeCN and water at 140 °C, but the M/L molar ratios of 1:2 and 5:3 give 2-D layered **3** and 3-D porous **4**, respectively. Complex **3** only contains doubly deprotonated Hdcbi, but complex **4** contains both doubly deprotonated Hdcbi and triply deprotonated dcbi. As for complex **5**, it is relatively complicated because of the incorporation of the co-ligand oxalate. However, it is clear that the presence of seven-coordinate Cd(II) and the inorganic Cd/O/N layer can be at least partly attributed to the incorporation of the coordinately flexible oxalate ligand.

It is also interesting to compare the coordination modes of the $H_n$dcbi ($n = 0-2$) species in **1**−**5**. As can be seen, the Cd(II) ions in the mononuclear and 1-D complexes such as **1**, **2**, and $[Cd(H_2dcbi)_2(H_2O)_2]$[10a] are generally coordinated by singly deprotonated H_2dcbi in monodentate, N,O-chelate, or bis-N,O-chelate mode (Scheme 1a, b, and d). In layered **3** and three-dimensional **4** and **5**, the Cd(II) ions are coordinated by doubly deprotonated Hdcbi, triply deprotonated dcbi, or both. Generally, the doubly deprotonated Hdcbi can bridge two to four Cd(II) ions (Scheme 1d, g, and h), while the triply deprotonated dcbi can bridge as many as five Cd(II) ions (Scheme 1l).

Complex **6** was synthesized in aqueous acetonitrile solution, and interestingly, the cyanide was formed in situ during the reaction. The in situ formation of cyanide under hydro(solvo)thermal conditions has been documented in several complexes, and the proposed possible mechanisms include an oxidization−desulfation reaction of thiocyanate[15] and the acid-catalyzed decomposition of isonicotinic acid.[16] In contrast, the cyanide in **6,** possibly, came from the decomposition of acetonitrile via C−C bond cleavage.

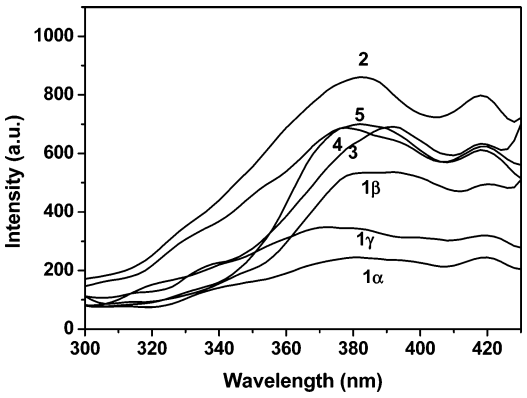

Figure 8. Photoluminescent spectra of **1**−**5** excited at 225 nm.

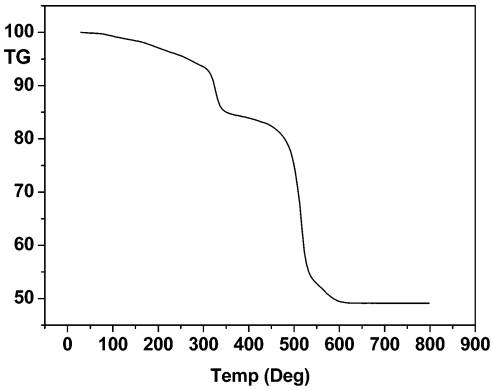

Figure 9. TGA curves of **4**.

Photoluminescence. The free H_3dcbi ligand shows very weak luminescence (almost cannot be detected) in the solid state at ambient temperature upon photoexcitation with ultraviolet light of 225 nm. However, complexes **1**−**5** exhibit strong violet blue photoluminescent emission with maxima in the range of 376−389 nm. The luminescence in the Zn(II) and Cd(II) complexes has been reviewed by Zheng and Chen,[17] and their studies reveal that, if the ligand is a heterocylic aromatic ligand, the heteroatom can effectively decrease the π and π^* orbital energies. Thus, the HOMO and LUMO of the complexes may lack the contribution from metal atoms, and the LMCT emission can be excluded; the nature of the organic ligand will play a critical role in the photoluminescence mechanism of the Zn(II) and Cd(II) complexes. The similarity of the emission and excitation spectra for **1**−**5** is in agreement with the explanation, which indicates that a ligand-centered $\pi \rightarrow \pi^*$ excitation is responsible for emissions in **1**−**5**. The intensity increase of the luminescence when coordinated to Cd(II) ions may be attributed to the chelation of the $H_n$dcbi ligand to the Cd(II) center, which increases the rigidity of $H_n$dcbi and reduces the nonradiative relaxation process.

(15) (a) Zhang, X.-M.; Fang, R.-Q.; Wu, H.-S. *J. Am. Chem. Soc.* **2005**, *127*, 7670. (b) Zhang, X.-M.; Hao, Z.-M.; Wu, H.-S. *Inorg. Chem.* **2005**, *44*, 7301.

(16) Kang, Y.; Yao, Y.-G.; Qin, Y.-Y.; Zhang, J.; Chen, Y.-B.; Li, Z.-J.; Wen, Y.-H.; Cheng, J.-K.; Hu, R.-F. *Chem. Commun.* **2004**, 1046.

(17) (a) Zheng, S.-L.; Chen, X.-M. *Aust. J. Chem.* **2004**, *57*, 703. (b) Zheng, S.-L.; Yang, J.-H.; Yu, X.-L.; Chen, X.-M.; Wong, W. T. *Inorg. Chem.* **2004**, *43*, 830.

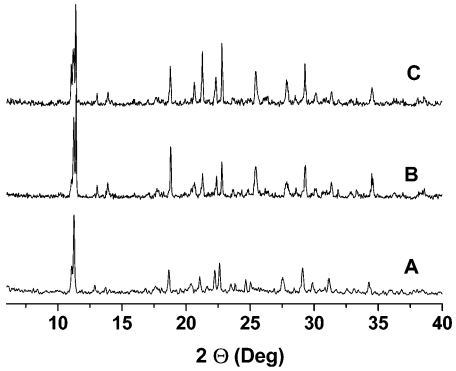

Figure 10. XRPD of as-synthesized (A), calcinated at 200 °C for 5 h (B), and calcinated at 250 °C for 5 h (C) complex **4**.

XRPD and TGA. To study the microporosity chemistry of **4**, thermogravimetric analysis in air and under 1 atm of pressure at a heating rate of 10 °C min^{-1} was performed on a polycrystalline sample, which showed multistep weight loss in the temperature of 60−600 °C (Figure 9). The initial weight loss of 8.8% in the temperature range of 60−300 °C corresponds to the removal of solvent water molecules, and the release of the water molecules up to a high temperature is attributed to the strong cooperative H-bonding interaction between the coordinated and solvent water molecules and to the relatively small one-dimensional channel. The final residue of 49% is in agreement with the percentage of CdO in **4**. As-synthesized complex **4** was calcinated in air at 200 and 250 °C for 5 h, and the XRPD patterns of the resulting products are similar to those of as-synthesized **4.** Elemental microanalysis of **4** after calcination (C 20.02, H 0.76, N, 9.33; Calcd C 20.11, H 0.68, N 9.38) in air at 250 °C for 5 h shows that the solvent water molecules are removed in the course of calcination, and all these indicate that the porous network of **4** remains after the calcination at 250 °C and removal of guests. When the calcination of **4** was performed at 300 °C for 5 h, the XRPD patterns indicate that network of **4** collapsed.

Conclusion

Fine control over synthetic conditions such as stoichiometry, solvent, and pH value generated seven complexes of metal 4,5-imidazoledicarboxylates which show structures ranging from mononuclear, one-dimensional, and two-dimensional to a three-dimensional microporous framework. Analyses of synthetic conditions, structures, and coordination modes of $H_n$dcbi reveal that the solvent and M/L molar ratio are two very important factors to products and coordination modes of $H_n$dcbi. Seven coordination modes of $H_n$dcbi ranging from monodentate to μ_5 have been observed, among which four modes are first found. The study reveals that the singly deprotonated H_2dcbi generally coordinates in the monodentate imidazole-N or N,O-chelate mode to result in mononuclear structures, the doubly deprotonated Hdcbi can coordinate in μ_2, μ_3, or μ_4 mode to generate one-dimensional or two-dimensional structures, and the triply deprotonated dcbi can coordinate in different μ_5 modes to form three-dimensional structures. The study also reveals that cyanide can occastionally be formed in situ by C−C bond cleavage of organonitrile. The photoluminescent emissions of the five cadmium complexes further show that the nature of heterocylic aromatic ligands plays a critical role in the photoluminescence mechanism of Cd(II) complexes. The microporous network of **4** can be retained up to 250 °C in the absence of guest water molecules.

Acknowledgment. This work was financially supported by NSFC (20401011), the Foundation for the Author of National Excellent Doctoral Dissertation of PR China (200422), and the Youth Foundation of Shanxi (20041009).

Supporting Information Available: Crystal structural data for **1**−**7** in CIF format and figures showing the packing arrays and simulated XRPD patterns This material is available free of charge via the Internet at http://pubs.acs.org.

IC052099M